

Goal-directed whisking increases phase-locking between vibrissa movement and electrical activity in primary sensory cortex in rat

Karunesh Ganguly* and David Kleinfeld*^{†‡§}

[†]Department of Physics, [‡]Center for Theoretical Biological Physics, and ^{*}Graduate Program in Neurosciences, University of California, La Jolla, CA 92093

Edited by Charles F. Stevens, The Salk Institute for Biological Studies, La Jolla, CA, and approved June 29, 2004 (received for review December 20, 2003)

We tested the hypothesis that behavioral context modulates phase-locking between rhythmic motor activity and concomitant electrical activity induced in primary sensory (S1) cortex. We used exploratory whisking by rat as a model system and recorded two measures: (i) the mystacial electromyogram (∇ EMG) as a surrogate of vibrissa position, and (ii) the field potential (∇ LFP) in S1 cortex as an indicator of electrical activity. The degree to which the ∇ EMG and ∇ LFP were phase-locked was compared for three categories of rhythmic whisking: (i) searching for an object with the vibrissae for a food reward, (ii) whisking in air for the goal of returning to the home cage, and (iii) whisking with no reward. We observed that the magnitude of phase-locking was nearly tripled for the two rewarded conditions compared to unrewarded whisking. Critically, increased locking was not accompanied by an increase in the amplitude of the cortical ∇ LFP for the rewarded tasks. Additional experiments showed that there was no significant relation between the amplitude of a sensory-evoked response in S1 cortex and the magnitude of the locking between the ∇ EMG and the ∇ LFP during whisking. We conclude that the behavioral context of a whisking task can increase the modulation of S1 cortical activity by motor output without a concomitant increase in the magnitude of activity.

Tactile somatosensation can be classified as either active or passive based on the presence or absence of voluntary movements. Past studies suggest that the sensory processing that underlies active sensation is different from that of passive touch (1–3). In particular, active touch appears to require integration of both sensory and motor information (4, 5). The rat mystacial macrovibrissae are a part of an active somatosensory system. Rodents rhythmically sweep their vibrissae during exploration (6–9), spatial localization tasks (10–12), and tactile discrimination tasks (13–15). As an active sensory system, the motion of the sensors must be taken into account as tactile sensory inputs are processed.

The experiments of Hutson and Masterson (10) provide evidence that vibrissa primary somatosensory (S1) cortex is required for sensorimotor integration during whisking tasks. Through behavioral tests on rats with ablated versus intact vibrissa S1 cortices, they concluded that S1 cortex is not required for the perception of passive touch but is essential for tasks, such as the detection of a distant platform across a gap, that require active palpation with the vibrissae. Thus, S1 cortex is a critical component of computations to detect stimuli that are encountered during active motion of the vibrissae. Consistent with this interpretation are electrophysiological findings that demonstrate that unit activity in vibrissa S1 cortex (7), as well as the field potential (8), is weakly phase-locked to vibrissa motoneuron output as rats whisk in search of a food tube. These data imply that vibrissa S1 cortex receives a “reference signal” linked to the position of the vibrissae. Such a representation of motor activity in sensory cortex is likely, although not proven, to be involved in computations to detect and localize vibrissa contacts during the active movement of the vibrissae (16, 17). Thus, the extent of phase-locking between the sensory reference signal and motor output to the vibrissae is a measure of the ability of S1 cortex to predict vibrissa position based on the sensory input stream.

Here we ask whether phase locking between the sensory reference signal and motor output can be influenced by altering the behavioral context in which whisking is generated. Two findings led to the present experiments. First, the work of Platt and Glimcher (18) showed that the probability of directed eye movements in monkey, as well as the extent of spike activity in a sensorimotor area of cortex, was tied to the expectation of a reward. Second, reward is a particularly salient event that leads to heightened attention (19). In primates, attention to a somatosensory stimulus led to an increased spike rate (20, 21) and to an increase in the synchrony of spiking (22) among cells in somatosensory cortex when compared with the case of inattention. Thus, it is likely that reward that is contingent on whisking will modulate cortical activity related to whisking. However, *a priori*, it is not obvious whether the overall level of electrical activation of S1 vibrissa cortex is changed as opposed to the part of the cortical response that is phase-locked to whisking.

The spectral coherence between rhythmic motor output to the vibrissae and the reference signal in S1 cortex served to quantify the extent of phase-locking. We compared this sensorimotor coherence under behavioral conditions in which whisking was either rewarded or unrewarded. In one reward-based task, denoted the “contact task,” we trained rats to reach across a gap and actively palpate a piezoelectric tactile stimulus. Vibrissa contact led to an immediate food reward. Whereas the contact task was specifically designed to assess coherence during active palpation, we constructed a second task to assess coherence during reward-based whisking in the absence of contact or food. These experiments capitalized on the demonstration that behavioral training can be achieved when access to the home cage is used for motivation (23, 24). This task, denoted the “home task,” required that the animal whisk in air, for which it was rewarded by narrowing the gap that it needed to cross so that it could return to its home cage.

Methods

Behavioral Training and Automation. Three Long-Evans female rats (Charles River Breeding Laboratories), 200–250 g initial weight, served as subjects for the extracellular measurements. Six additional rats served as subjects to optimize the behavioral tasks. All animals were habituated to human touch and to the behavioral platform (Fig. 1A) for a period of 2–3 weeks. The outside dimensions of the platform were 460 × 485 mm, the walkway was 76 mm across, and the perch extended 89 mm. The rats were then trained for 2–3 weeks to perform the contact task, where the animals must stretch across a gap and contact a tactile stimulus (Fig. 1B). The stimulus consisted of a periodic array of piezoelectric wafers (LDT0–028K; Measurement Specialties, Fairfield, NJ) that doubled as a contact

This paper was submitted directly (Track II) to the PNAS office.

Abbreviations: S1, primary somatosensory; EMG, electromyogram; LFP, field potential; SDM, standard deviation of the mean.

[§]To whom correspondence should be addressed. E-mail: dk@physics.ucsd.edu.

© 2004 by The National Academy of Sciences of the USA

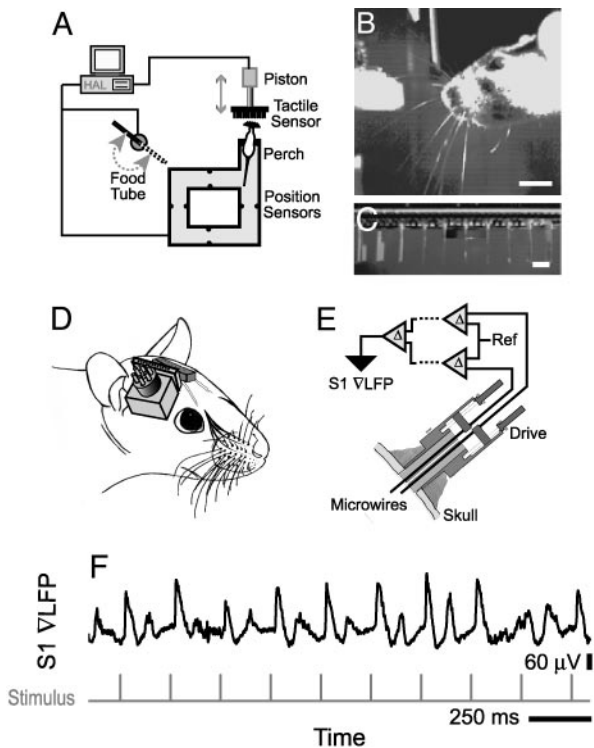


Fig. 1. Overall setup of the experiment. (A) Schematic of the behavioral platform and robotics. Pairs of infrared LED/photodiodes detect when the rat moves on the platform or cranes across the gap. The latter signal is used to advance the tactile stimulus by 3 cm and thus enable contact of one or more vibrissae with an array of piezoelectric wafers. Successful contact leads to delivery of liquid diet through a food tube. (B) Video image of a rat as it cranes and actively palpates the piezoelectric wafers, configured as the tactile stimulus, during the task. (Scale bar, 15 mm.) (C) Video image of the piezoelectric wafers. (Scale bar, 0.762 mm.) (D) Schematic of a rat with microwires placed in the mystacial pad to record EMG signals and a microdrive placed over vibrissa S1 cortex as a means to position microwires into a local region of cortex. (E) Schematic of the microdrive and signal processing. (F) A continuous record of the evoked potentials in response to periodic puffs to the vibrissa D3, the principal vibrissa, with the rat anesthetized with ketamine/xylazine.

detector (25). They were mounted on a circuit board at 0.30-inch spacing (Fig. 1C) and attached to a pneumatic piston that presented and retracted the stimulus (Fig. 1A).

Each trial began with presentation of the stimulus. The rats were required to repeatedly contact the stimuli for a period of 1–3 s to receive a liquid food reward (0.2 ml per trial; LD-100; PMI Feeds, St. Louis) from the food tube. They received only water, ad libitum, outside of training. The occurrence of a sufficient number of whisker contacts was followed by the retraction of the tactile stimuli and presentation of the food tube (Fig. 1A). Onset and duration of vibrissa contacts were monitored by custom software (LABVIEW v5.1; National Instrument, Dallas) that triggered stimuli retraction and activation of the food delivery. During the training period, the distance of the tactile stimuli from the edge of the perch was increased after each block of successful trials. This pattern continued until a distance was reached, between 120 and 150 mm, where the rats could only touch the stimulus with their macrovibrissae. The training period was complete only after the rats were able to successfully palpate the stimulus for at least 1 s with their vibrissae.

In addition to the contact task, we designed a home task to assess sensorimotor signaling during free but purposeful whisking before the onset of vibrissa contacts. At the end of a block of successful contact trials, the cage was presented next to the platform but at a distance that was out of the range of contact.

Without exception, the rats moved within <1–2 s to the edge of the platform and oriented their whisking toward the home cage (see Fig. 5A). After a variable time period, 2–40 s, the cage was moved within reach of the vibrissae. After the vibrissae contacted the cage, the rats invariably crossed into their home cage.

Chronic Electrophysiological Recordings. Vibrissa motion was assessed by electromyogram (EMG) recordings from 50- μ m-diameter microwires that were implanted across the mystacial pad, as described (9) (Fig. 1D). The final signal was calculated as the difference between two of the mystacial pad wires and is designated the ∇ EMG. This signal was observed to be essentially free from chewing, shivering, and other motor artifacts. The electrical activity in the vibrissa S1 cortex was measured by using 50- μ m-diameter microwires that were positioned by a microdrive array that was affixed to the skull, as described (7, 26). The field potential (∇ LFP) was calculated as the difference between the signals from a pair of electrodes separated by 450 μ m. Details of the signal conditioning (7–9) are given in the supporting information, which is published on the PNAS web site. To confirm that our ∇ LFP electrodes were correctly placed in vibrissa sensory cortex, we showed that brief puffs of air to a vibrissa evoked a ∇ LFP with the animal under anesthesia (Fig. 1F). The vibrissa that produced the largest ∇ LFP was considered the principal vibrissa.

After a 7- to 10-day postsurgical recovery period, the rats were placed on the behavioral platform and allowed to rehabilitate to the maze and the recording apparatus and to relearn the contact and home tasks for a period of 3–5 days. During this period, they were allowed to perform the contact task to receive the food reward.

Electrical Recording and Analysis. Whisking epochs of 1-s duration during the contact task were identified based on the contact signal from the piezoelectric sensors and an electrical signal from the infrared position sensor on the perch (Fig. 1A). Furthermore, such whisking was recorded with high-speed videography synchronized to the electrophysiology (9). Whisking epochs during the home task were only collected from the time of presentation of the home cage to the time at which the cage was moved closer. This ensured that whisking was free of contacts with external objects. Task-unrelated whisking was defined as whisking behavior with significant EMG activity during time periods when the rat was not performing either the contact or home tasks. Movement of the rat on the maze was observed by using standard videography of the platform and 910-nm illumination, and the onset of whisking was time-stamped.

Vibrissa Perturbation During Behavior. To determine whether changes in the sensorimotor coherence were linked to gating of incoming sensory input, we monitored the amplitude of air-puff-evoked responses. Pulses of air, 10 ms in duration at a 3- to 4-Hz repetition rate, were administered through a lightweight, mobile delivery system mounted on the rat's head (see Fig. 6A). This allowed us to compare variations in the air-puff-evoked response with that of the sensorimotor coherence in the whisking band.

Air-puff evoked ∇ LFP responses were parameterized in terms of the amplitude of their projection onto the trial-average response, a scalar measure denoted as $P_{\nabla\text{LFP}}^{(i)}$. We denote $V^{(i)}(t)$ as the ∇ LFP measured within a temporal window that encompassed the i th stimulus and form $\delta V^{(i)}(t) = V^{(i)}(t) - (1/T_{\text{epoch}}) \int_{\text{epoch}} dt V^{(i)}(t)$. The trial-averaged response is $\langle \delta V(t) \rangle = (1/N) \sum_{i=1}^N \delta V^{(i)}(t)$, where N is the number of stimuli in an epoch, and the projected amplitude for the response on a given trial is $P_{\nabla\text{LFP}}^{(i)} \equiv \int_{\text{epoch}} dt \delta V^{(i)}(t) \langle \delta V(t) \rangle / \int_{\text{epoch}} dt \langle \delta V^{(i)}(t) \rangle^2$.

Results

Brain activity was inferred from the differential local field potential in vibrissa S1 cortex (∇ LFP) (Fig. 1E), which probed the aggregate electrical activity in a $\approx 0.1\text{-mm}^3$ region of cortex

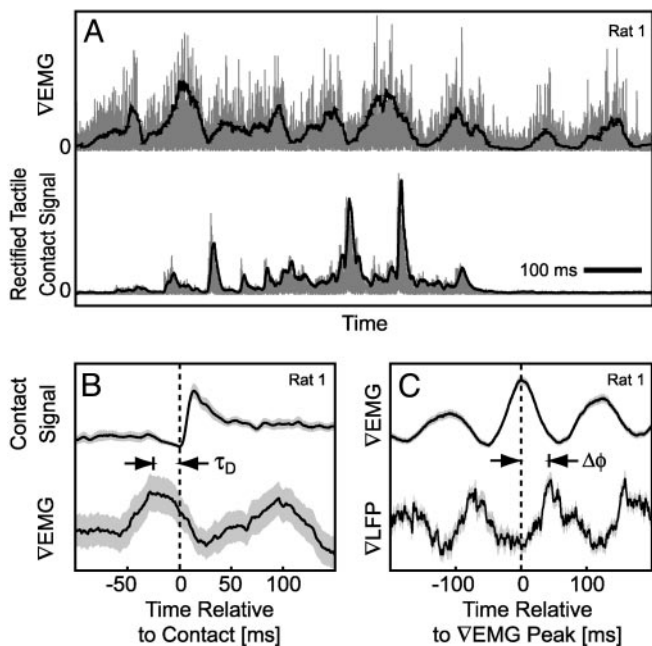


Fig. 2. The mystacial ∇ EMG and ∇ LFP signal from S1 cortex are phase-locked during palpation of a tactile stimulus during the contact task. (A) Single epoch of the rectified, mystacial ∇ EMG and the concomitant contact signal from the piezoelectric wafers. The gray traces represent the rectified voltage output from the ∇ EMG and the wafers. The dark lines represent the low-pass-filtered signals. (B) Contact triggered average ($n = 80$ trials) of the simultaneously recorded contact and ∇ EMG signals. The zero time point was defined as a positive change in slope of the contact signal. The black line is the mean, and the gray band is the ± 1 standard deviation of the mean (SDM), computed over all trials. The onset of contact is delayed relative to the peak of the EMG signal by τ_D . (C) The ∇ EMG-triggered average ($n = 93$), where time-zero is defined as the positive peak of the ∇ EMG, of the simultaneously recorded ∇ LFP and ∇ EMG signals. The ∇ LFP is phase-locked to the ∇ EMG signal with a phase-lag of $\Delta\phi$.

(Methods). This volume is estimated to contain 10^4 neurons (27). Our measure of motor activity was inferred from recordings of the EMG across the mystacial pad (∇ EMG) (Fig. 2A) and supplemented with videographic records of vibrissa movement. Contact of the vibrissae with a tactile stimulus was quantified through the use of piezoelectric wafers that served as both stimuli and sensors of single vibrissa contact (Fig. 1A–C).

Whisking with Reward Based on Contact. Rats were trained to crane their head across a gap and palpate a tactile stimulus with their vibrissae (Fig. 1A–C). We moved the tactile stimulus forward, so that it was accessible across the gap, after a variable 30- to 60-s period that followed completion of a previous trial. Contact led to a liquid food reward. Each trial consisted of a 1- to 5-s epoch of rhythmic whisking with contact, after which the tactile stimulus was retracted. To ensure that the rat walked around the behavioral apparatus between trials, we delayed the start of a new trial if sensors on the apparatus indicated that the animal lingered near the gap (Fig. 1A).

We examined the relationship between the position of the vibrissae and the ∇ EMG signal during the contact task. Videography showed that only the macrovibrissae made contact with the piezoelectric wafers (Fig. 1C). The ∇ EMG was correlated with the electrical signal from contact (Fig. 2A), which verifies that animals rhythmically palpated the stimulus. The contact triggered average of the ∇ EMG shows that the onset of contact lags the peak of the ∇ EMG (Fig. 2B). The value of the lag, $\tau_D \approx 25$ ms, is consistent with the results of past experiments that

demonstrated that the position of the vibrissae lags that of the ∇ EMG (9, 28).

Recordings from vibrissa S1 cortex exhibit rhythmic activity during the contact task. Of interest, the ∇ EMG-triggered ∇ LFP displayed a strong oscillatory signal that was phase-locked to the vibrissa motion during active contacts with the piezoelectric wafers (Fig. 2C). Thus, during active palpation of an object, there was a strong cortical signal that was phase-locked to the motion of the vibrissae.

Increased Coherence for Contact Task (Rewarded) Versus Task-Free (Unrewarded) Whisking. The contact task pairs a food reward with whisking. In contrast, unrewarded whisking occurred while our rats explored the behavioral platform between epochs of the contact task. We used data collected under both categories of whisking to quantify the impact of the different behavioral context on the coherence between the motor activity and the cortical electrical activity. Our measure was the spectral coherence, denoted $C(f)$, between the ∇ LFP and the ∇ EMG. The magnitude of $C(f)$ in the spectral band for whisking is the fraction of the ∇ LFP that is modulated by the ∇ EMG, with $0 < |C(f)| < 1$. Thus, the value of $|C(f)|^2$ in each frequency band plays a role analogous to the squared scalar correlation coefficient, r^2 , in regression analysis (ref. 29 and supporting information). The phase of $C(f)$ within this band reports the relative timing difference between the ∇ LFP and the ∇ EMG.

Example data illustrate key aspects of our results (rat 2). Measurements during the 1- to 5-s interval of rhythmic whisking with contact displayed high levels of sensorimotor coherence in the 7- to 11-Hz spectral band of whisking (Fig. 3A). In contrast, during unrewarded whisking, peaks in the sensorimotor coherence are barely discernable (Fig. 3B), but the ∇ EMG, and thus the amplitude of whisking, was as strong or stronger than in the contact task (compare ∇ EMG traces in Fig. 3B with those in A). Thus, qualitatively, the magnitude of the coherence can vary independently of the amplitude of whisking.

We calculated the trial-averaged spectral coherence for each category of whisking and consider first the results for one animal (rat 1). The trial-averaged coherence at the whisking frequency band during unrewarded whisking was $|C(f)| = 0.22 \pm 0.03$ (mean \pm SDM; $n = 111$ trials). This value rose to 0.52 ± 0.03 ($n = 66$ trials) during the contact task (Fig. 3C). Thus, the magnitude of the spectral coherence was significantly higher for rewarded versus unrewarded epochs of whisking. Lastly, in both cases the average phase at the whisking band was similar.

In the presence of noisy baseline activity whose spectrum overlaps with either the ∇ EMG or the ∇ LFP, an increased coherence between these two signals can arise from an increase in the signal-to-noise ratio of one or both signals (Appendix). Interestingly, we observed that the power in the ∇ EMG throughout the whisking band is statistically unchanged ($P > 0.05$) during epochs of the contact task as compared to unrewarded whisking (Fig. 3D). Furthermore, the power in the ∇ LFP throughout the whisking band is lower and less variable, albeit not significantly so, during the contact trials as opposed to unrewarded whisking (Fig. 3E). Thus, to the extent that baseline fluctuations are unchanged by the behavioral context, the increased coherence does not result from an increase in electrical activity in cortex.

Population data across all three animals showed a large and consistent increase in the magnitude of the coherence for whisking during the contact task, with high statistical confidence ($P < 0.02$) (Fig. 3F). Furthermore, the increase occurred in the absence of a systematic change in the spectral power of the ∇ EMG (Fig. 3G), but in the presence of a decrease in the power in the ∇ LFP (Fig. 3H).

What is the basis of the higher coherence for reward dependent whisking? A scatter plot of the magnitude of the coherence at the center of the whisking frequency band, as a function of integrated spectral power of the ∇ EMG in the same band, shows

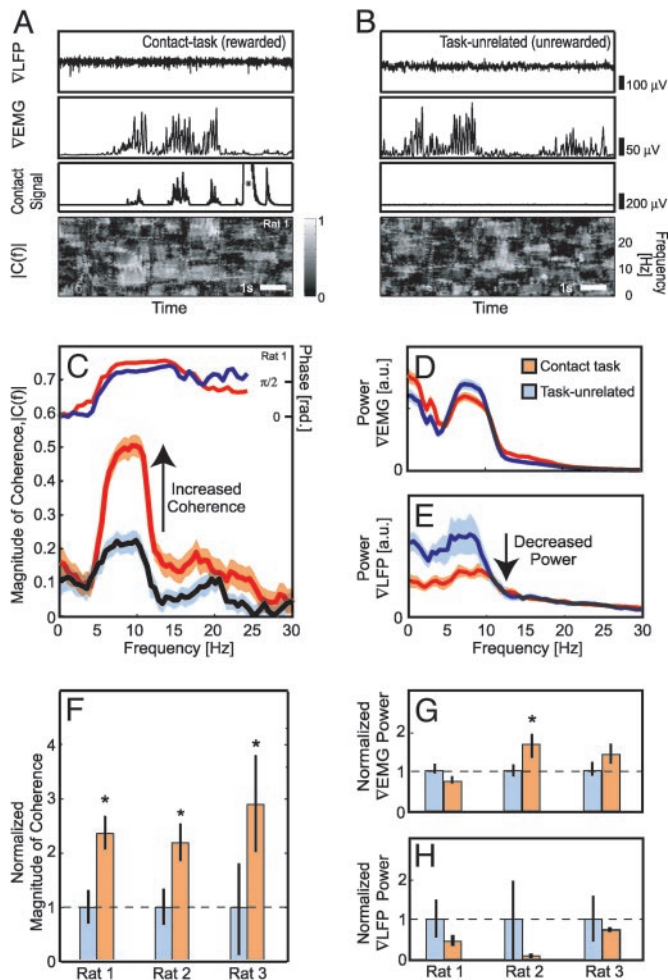


Fig. 3. Differences in the response of the rat during the rewarded, contact task versus unrewarded, task-independent whisking. (A) Representative data trace in the contact task. (Top) The ∇ LFP in S1 cortex. (Upper Middle) The mystacial ∇ EMG. (Lower Middle) The occurrence of contacts of the vibrissae with the tactile stimuli; the asterisk after the contact events indicates a detector artifact at the time of retraction of the stimulus. (Bottom) The magnitude of the spectral coherence, $|C(f)|$, between the ∇ LFP and the ∇ EMG across the trial; $C(f)$ was computed in a 1-s sliding window with a bandwidth of 2.5 Hz and a step size of 20 ms. (B) Representative trace during unrewarded whisking. Panels are as in A; in this trial, the stimulus is not approached and thus there is no contact signal. (C) The magnitude and phase of the spectral coherence, $C(f)$, between the ∇ LFP and the ∇ EMG for the contact task (red) versus unrewarded whisking (blue) for a single rat. The solid lines are the mean, and the transparent bands are ± 1 SDM, estimated over all trials. (D) The spectral power in the ∇ EMG during the contact task compared with unrewarded whisking for a rat. The two spectra are statistically indistinguishable at the 95% confidence level. (E) The spectral power in the ∇ LFP during the contact task compared with unrewarded whisking. The two spectra are statistically indistinguishable. (F) Tabulation of the average magnitude of the spectral coherence of the response for the peak during the two categories of whisking. In all cases (asterisk), the coherence during the contact task is significantly higher (* , $P < 0.02$) than that in unrewarded whisking. The bars are ± 2 SDM. (G and H) Tabulation of the relative power in the ∇ EMG and the ∇ LFP, respectively, averaged in the 7- to 10-Hz whisking band, across all three rats ($n = 66, 127,$ and 100 trials, respectively, for the contact task, and $n = 111, 195,$ and 160 trials, respectively, for the unrewarded whisking).

that there is a weak relation between $|C(f)|$ and the ∇ EMG (Fig. 4A). The trend for the contact trials is $r = 0.24$ ($P < 0.06$) and for the task-unrelated trials is 0.25 ($P < 0.02$); thus, the power in the ∇ EMG explains only a fraction $r^2 = 0.06$ of the increase in coherence. These data show that the 2- to 3-fold increase in

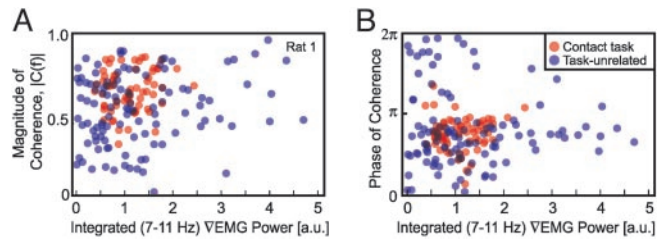


Fig. 4. Magnitude (A) and phase (B) of the spectral coherence between the ∇ LFP and the mystacial ∇ EMG as a function of the integrated power in the whisking band of the ∇ EMG. Data were obtained for a single rat during the contact task (red) and unrewarded whisking (blue).

the magnitude of the coherence during task-related whisking did not result from a simple increase in power of sensory input or motor output; equivalent results are found for all animals. On the other hand, the scatter plot for the phase of the coherence demonstrates that there is a larger spread in the distribution of phases for the unrewarded versus task-related whisking trials (Fig. 4B). Thus, the decreased variability in phase of the ∇ EMG versus the ∇ LFP between trials can explain the higher average sensorimotor coherence during the contact trials (Fig. 3C).

Increased Coherence for Home Task Versus Task-Free Whisking. The heightened coherence for the contact task could result from either the reward contingency or from contact *per se*. To discriminate among these possibilities, we considered a second task in which whisking was rewarded without the necessity for vibrissa contact. The coherence was calculated in a 2- to 40-s period of whisking that immediately preceded the movement of the cage to within reach of the vibrissae.

Example data illustrates key aspects of whisking as the rat craned her head across the gap during the home task (rat 2). As in the contact task, whisking behavior displayed high levels of sensorimotor coherence in the whisking frequency band (Fig. 5B). Furthermore, for the case of the home task, the coherence is sufficiently large toward the onset of the trial so that oscillations in the ∇ LFP that are locked to motor output, i.e., the ∇ EMG, are clearly visible (asterisk in Fig. 5B). Interestingly, $|C(f)|$ gradually wanes over time when home cage remains distant. We next quantified the trial-averaged spectral coherences for the home task and consider first the results for this animal. Although the trial-averaged coherence at the whisking frequency band during unrewarded whisking was $|C(f)| = 0.17 \pm 0.03$ ($n = 195$ trials), it increased to 0.45 ± 0.03 ($n = 88$ trials) during the home task (Fig. 5C). The average phase in the whisking band was very similar for both tasks (Fig. 5C).

Population data across all three rats showed a large and significant increase in the magnitude of the sensorimotor coherence for the home task (Fig. 5D). Furthermore, whisking behaviors during the home task displayed values of coherence that were similar to those for the contact task (compare Figs. 3F and 5D). Thus, the magnitude of the spectral coherence was systematically and significantly higher for tasks that rewarded whisking versus unrewarded epochs of whisking. As in the case of the home task, the increase in coherence was not accompanied by significant increases in the spectral power of either the ∇ EMG (Fig. 5E) or the ∇ LFP (Fig. 5F).

Metaanalysis. The coherence between cortical electrical activity and motor activity is a normalized measure. To the extent that the noise sources associated with the underlying signals are independent of the context of whisking, the coherence can depend on the overall amplitude of one or both signals (Appendix). For the one example of a significant increase in the ∇ EMG power (rat 2 in Fig. 3G), the normalized increase of $\nabla\text{EMG}_{\text{contact}}^{\text{rat1}} / \nabla\text{EMG}_{\text{task-unrelated}}^{\text{rat1}} = 1.6 \pm 0.3$ is too small to account for the normalized change in coherence of

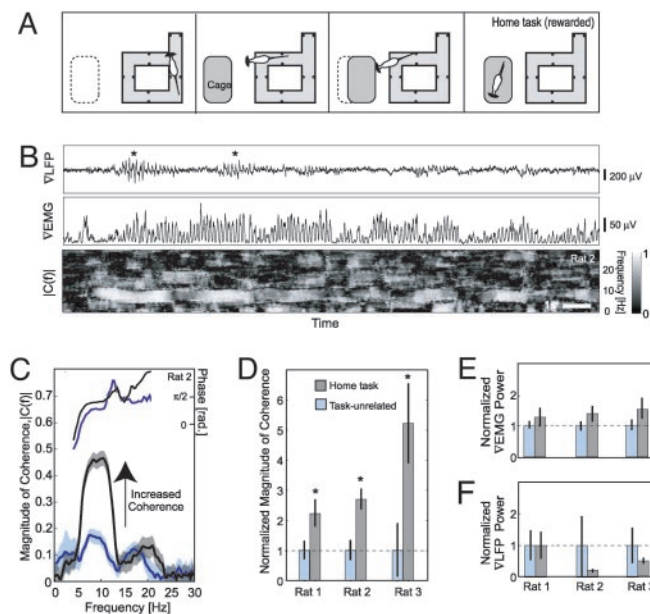


Fig. 5. The response of the rat during the home task as compared with unrewarded whisking. (A) Diagram displaying the setup for the home task, wherein the cage is introduced at a fixed position, initially spaced 20 cm from the platform, and then moved to within contact distance 2–40 s later. (B) Representative trace in the home task. (Top) The ∇ LFP. (Middle) The ∇ EMG. (Bottom) The magnitude of the spectral coherence, $|C(f)|$, between the ∇ LFP and the ∇ EMG across the trial; $C(f)$ was computed in a 1-s sliding window with a bandwidth of 2.5 Hz and a step size of 20 ms. (C) The magnitude and phase of the spectral coherence, $C(f)$, for the home task versus unrewarded whisking for a single rat. The solid line is the mean, and the transparent band is ± 1 SDM. (D) Tabulation of the average magnitude of the spectral coherence of the response for the peak during the two categories of whisking. In all cases, the coherence during the home task is significantly higher (*, $P < 0.02$) than that in unrewarded whisking. For rat 3 only, the coherence during the home task was significantly greater than that during contact ($P < 0.05$; see also Fig. 3F). The bars are ± 2 SDM. (E and F) Tabulation of the relative power in the ∇ EMG and ∇ LFP, respectively, averaged in the 7- to 11-Hz whisking band, across all three rats ($n = 22, 88$, and 83 trials, respectively, for the home task and $n = 111, 195$, and 160 trials, respectively, for the unrewarded whisking).

$|C_{\text{contact}}^{\text{rat1}}|/|C_{\text{task-unrelated}}^{\text{rat1}}| = 2.4 \pm 0.3$. As an average over both tasks and all animals, $\text{VEMG}_{\text{contact+home}}^{\text{all rats}}/\text{VEMG}_{\text{task-unrelated}}^{\text{all rats}} = 1.32 \pm 0.26$, which suggests a trend toward increased whisking amplitude in the goal-directed tasks (Figs. 3G and 5E), and $\nabla\text{LFP}_{\text{contact+home}}^{\text{all rats}}/\nabla\text{LFP}_{\text{task-unrelated}}^{\text{all rats}} = 0.50 \pm 0.16$, which indicates a significant decrease in the ∇ LFP for the rewarded tasks (Figs. 3G and 5E). In contrast, $|C_{\text{contact+home}}^{\text{all rats}}|/|C_{\text{task-unrelated}}^{\text{all rats}}| = 2.93 \pm 0.47$ as an average over tasks and animals, so that the magnitude of the normalized coherence is a factor of 2.2 times larger than the increase in the normalized ∇ EMG and nearly 6 times greater than the change in ∇ LFP. Thus the increase in coherence during goal-directed tasks is not the result of a possible change in signal amplitude during the tasks.

Gating of Sensory Input. Much of the activity in S1 cortex originates internally, as opposed to via sensory input (8). Thus a change in the ∇ LFP within the frequency range of whisking could mask a change in sensitivity in sensory input during the reward-based whisking tasks. To test this possibility, and as a means to acquire long stretches of continuous ∇ LFP and ∇ EMG data with a varying coherence, we used the home task (Fig. 6A) with the addition of rhythmic air puffs (Fig. 6A). We observed a stimulus-locked evoked potential that had a defined temporal pattern (Fig. 6B Left) and whose amplitude varied over time (Fig. 6B Right). If gating of the sensory stream occurs (2, 3,

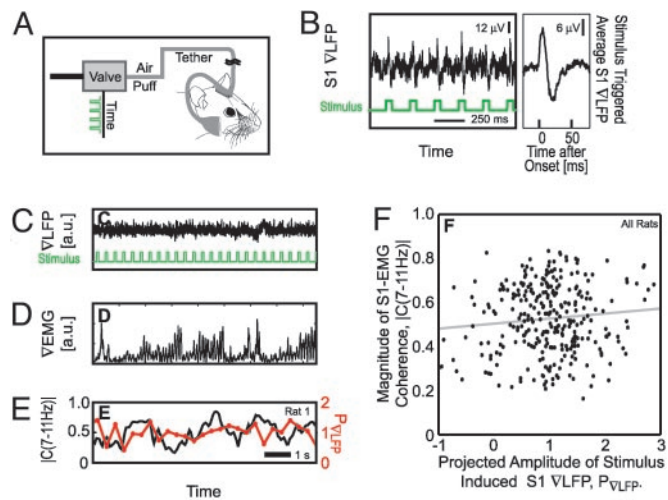


Fig. 6. Measurement of the spectral coherence between the ∇ LFP and the mystacial ∇ EMG, $|C(7-11 \text{ Hz})|$ as a function of the amplitude of the evoked ∇ LFP response, $P_{\text{VLF}}^{(i)}$. (A) The setup that is used to deliver air puff stimuli to the vibrissae during either the awake or the anesthetized condition. The frequency of air puffs was regulated through a train of digital pulses sent to the valve. (B) Evoked ∇ LFPs in response to periodic puffs in the awake, moving rat. (Left) A continuous record of responses and the right panel shows a stimulus triggered average over 200 stimuli. These traces are used to compute the projected amplitude in part F. (C–E) Representative traces during the home task with concurrent periodic stimulation of the vibrissae. (C) The ∇ LFP and the fiducials for the periodic stimuli. (D) The ∇ EMG. (E) Two measures on the data. First, the magnitude of the spectral coherence, averaged in the 7- to 11-Hz whisking band in 1-s windows during the home task, between the ∇ EMG and ∇ LFP. Second, the projected amplitude of the stimulus induced response. The projected amplitude of the response, $P_{\text{VLF}}^{(i)}$, was derived from the evoked ∇ LFP (B) after each stimulus (two animals with $n = 40$ and $n = 252$ measurements, respectively, obtained from 8-s epochs with 3-Hz stimulation). (F) The relation between the magnitude of the coherence and the normalized amplitude of the stimulus induced response in S1 cortex; the two signals are uncorrelated.

30–32), we posited that the coherence between the ∇ LFP and ∇ EMG would covary with the amplitude of the puff response.

We parameterized the puff response in terms of its projected amplitude, $P_{\text{VLF}}^{(i)}$ (Methods), which is a sensitive measure of the trial-to-trial variation of the evoked ∇ LFP. As a control, we observed no obvious interference or entrainment of normal whisking (see Figs. 5B and 6D). We then calculated the coherence between the ∇ LFP and ∇ EMG in a moving 1-s window. The magnitude of $C(f)$, after averaging over the spectral band for whisking, was compared with the projected amplitude of the puff evoked response (Fig. 6C–E). There was no significant correlation between the magnitude of the coherence and the value of the evoked response (Fig. 6F; $r = 0.10$ and $P > 0.05$).

Discussion

Our results show that the coherence between the electrical activity in vibrissa S1 cortex (∇ LFP) and the rhythmic movement of the vibrissae (∇ EMG) can vary with the behavioral context of the whisking. For unrewarded whisking epochs, the magnitude of the coherence was significantly nonzero, but small (Fig. 3C). In contrast, during a task in which rats actively palpated a distant tactile stimulus to trigger a food reward, the magnitude of the coherence in the band of whisking frequencies was more than double that for the unrewarded whisking epochs recorded within the same session (Fig. 3C). The observed increase was not limited to tasks in which the vibrissae were actively contacting an object. In a second task, designed to prolong goal-oriented exploratory whisking in the absence of contact and before reward, we observed that the magnitude was even more strongly

increased relative to the unrewarded whisking (Fig. 5C). The heightened coherence for the contact and home tasks, relative to unrewarded whisking (Figs. 3F and 5D), occurred without systematic increases in the underlying spectral power in the VEMG (Figs. 3G and 5E) and VLFP (Figs. 3H and 5F).

Reward or Attention? We categorized our behavioral paradigms in terms of expectation of reward-based tasks versus unrewarded whisking. Although we have focused on the role of reward, the behavioral situation associated with increased coherence is also characterized by postural changes, e.g., craning, and by shifts in attention. Changes in coherence between unit activity in motor cortex, as opposed to sensory cortex in the present work, and the underlying tremor in motoneuron output have been observed for hand muscles in monkey during a precision grip task (33, 34). Although the underlying mechanism for either effect is unknown, modulators of cortical excitability could increase the extent of phase-locking, perhaps controlled by thalamic-induced gain control (35) or synchrony across cortex (36, 37).

Past studies have shown that attention can regulate the timing or synchrony of neuronal responses in sensory cortex, as opposed to the rate of spiking. Steinmetz *et al.* (22) maintained a tactile stimulus on a digit in the monkey and measured the spike response in somatosensory cortex because the animal performed a visual task versus a tactile discrimination task. In the latter case, many units in primary and secondary areas of somatosensory cortex displayed a strong increase in synchrony. A conceptually similar, albeit weaker, effect is observed in different areas of visual (38) and visual-motor (39) cortex in monkey when foveation is used as a means to direct attention. The present work is complementary to these past efforts. The studies with monkeys involved manipulations of attention on a trial-by-trial basis, whereas in the rat experiments, we could only change the reward contingency on the scale of many blocks of trials. In our study, attention is neither explicitly manipulated, nor is there any measure of either attention or cortical arousal. Nonetheless, our behavioral paradigm involved an active rhythmic sensory task. This afforded us the unique opportunity to quantify synchrony in terms of a measure of coherence with motor output.

Sensorimotor Integration. It is conjectured that a central role of vibrissa primary sensory cortex is to compute the position of contact of the vibrissae with tactile stimuli in head-centered coordinates (16, 17, 40). This computation requires a reference signal of vibrissa position (7, 41). Recent work provides evidence

that, during rhythmic whisking, such a computation could be performed by the multiplication of the sensorimotor reference signal with a contact signal (42). The strength of the resultant output signal could be expected to be proportional to the sensorimotor coherence in the whisking band. Thus, correlated activity serves to select the relevant population of neurons, as proposed for perceptual discriminations tasks (43–45). Furthermore, judicious processing of correlated signals can lead to the removal of common sources of fluctuations (46). Within this scenario, the modulation in coherence found in the present work provides a means to generate a reliable motor command that influences the heading and locomotion of the animal based on the saliency of environmental cues.

Appendix: Coherence in the Presence of Stationary Additive Noise

We denote the two signals as $V(t)$ and $U(t)$, and assume that each is the sum of an idealized signal, denoted $v(t)$ and $u(t)$, respectively, and a noise term. Thus $V(t) = v(t) + \eta_v(t)$ and $U(t) = u(t) + \eta_u(t)$, where the noise sources $\eta_v(t)$ and $\eta_u(t)$ are independent with zero mean and spectral variances $\sigma_v^2(f)$ and $\sigma_u^2(f)$, respectively. The spectral coherence is defined as $C(f) \equiv \langle \tilde{V}(f)\tilde{U}^*(f) \rangle / \sqrt{\langle |\tilde{V}(f)|^2 \rangle \langle |\tilde{U}(f)|^2 \rangle}$, where $\langle \dots \rangle$ denotes averaging over all degrees of freedom. Thus

$$C(f) = \frac{\langle \tilde{v}(f)\tilde{u}^*(f) \rangle}{\sqrt{\langle |\tilde{v}(f)|^2 \rangle \langle |\tilde{u}(f)|^2 \rangle}} \sqrt{\frac{\text{SNR}_v^2(f)}{1 + \text{SNR}_v^2(f)} \frac{\text{SNR}_u^2(f)}{1 + \text{SNR}_u^2(f)}} \quad [1]$$

where $\text{SNR}_v(f) = \sqrt{\langle |\tilde{v}(f)|^2 \rangle} / \sigma_v(f)$ and $\text{SNR}_u(f) = \sqrt{\langle |\tilde{u}(f)|^2 \rangle} / \sigma_u(f)$ are the signal-to-noise ratios (SNRs) associated with $V(t)$ and $U(t)$, respectively, and $\langle \tilde{v}(f)\tilde{u}^*(f) \rangle / \sqrt{\langle |\tilde{v}(f)|^2 \rangle \langle |\tilde{u}(f)|^2 \rangle}$ is the value of $C(f)$ in the limit of infinite SNRs. At low SNRs, multiplying $v(t)$ or $u(t)$ by a scalar changes the value of $C(f)$; this effect is linear in the limit of low SNR, for which $C(f) \approx \langle \tilde{v}(f)\tilde{u}^*(f) \rangle / \sqrt{\sigma_v^2(f) \sigma_u^2(f)}$.

We thank Earl Dolnick for assistance with the electronics and Rune W. Berg, Theodore H. Bullock, John C. Curtis, Ford F. Ebner, Beth Friedman, Herbert Levine, Samar B. Mehta, Partha P. Mitra, John H. Reynolds, and H. Phillip Zeigler for discussions. This work was supported by National Institute of Mental Health Grant MH59867, and the National Science Foundation Integrative Graduate Education and Research Traineeship Program.

- Chapman, C. E. (1994) *Can. J. Physiol. Pharmacol.* **72**, 558–570.
- Chapin, J. K. & Woodward, D. J. (1982) *Exp. Neurol.* **78**, 670–684.
- Chapin, J. K. & Woodward, D. J. (1982) *Exp. Neurol.* **78**, 654–669.
- Aoki, F., Fetz, E. E., Shupe, L., Lettich, E. & Ojemann, G. A. (2001) *Biosystems* **63**, 89–99.
- Braun, C., Heinz, U., Schweizer, R., Wiech, K., Birbaumer, N. & Topka, H. (2001) *Brain* **124**, 2259–2267.
- Welker, W. I. (1964) *Behavior* **12**, 223–244.
- Fee, M. S., Mitra, P. P. & Kleinfeld, D. (1997) *J. Neurophysiol.* **78**, 1144–1149.
- O'Connor, S. M., Berg, R. W. & Kleinfeld, D. (2002) *J. Neurophysiol.* **87**, 2137–2148.
- Berg, R. W. & Kleinfeld, D. (2003) *J. Neurophysiol.* **89**, 104–117.
- Hutson, K. A. & Masterton, R. B. (1986) *J. Neurophysiol.* **56**, 1196–1223.
- Harris, J. A., Petersen, R. S. & Diamond, M. E. (1999) *Proc. Natl. Acad. Sci. USA* **96**, 7587–7591.
- Shuler, M. G., Krupa, D. J. & Nicolelis, M. A. (2002) *Cereb. Cortex* **12**, 86–97.
- Brecht, M., Preilowski, B. & Merzenich, M. M. (1997) *Behav. Brain Res.* **84**, 81–97.
- Carvell, G. E. & Simons, D. J. (1990) *J. Neurosci.* **10**, 2638–2648.
- Guic-Robles, E., Valdivieso, C. & Guajardo, G. (1989) *Behav. Brain Res.* **31**, 285–289.
- Ahissar, E. & Kleinfeld, D. (2003) *Cereb. Cortex* **13**, 53–61.
- Mehta, S. B. & Kleinfeld, D. (2004) *Neuron* **41**, 181–184.
- Platt, M. L. & Glimcher, P. W. (1999) *Nature* **400**, 217–218.
- Bushnell, P. J. (1998) *Psychopharmacology* **138**, 231–259.
- Nelson, R. J. (1984) *Brain Res.* **304**, 143–148.
- Hsiao, S. S., Johnson, K. O. & O'Shaughnessy, D. M. (1993) *J. Neurophysiol.* **70**, 444–447.
- Steinmetz, P. N., Roy, A., Fitzgerald, P. J., Hsiao, S. S., Johnson, K. O. & Niebur, E. (2000) *Nature* **9**, 187–190.
- Premack, D. & Shanab, M. E. (1968) *Nature* **125**, 288–289.
- Masuda, Y., Odashima, J. I., Murai, S., Saito, H., Itoh, M. & Itoh, T. (1994) *Physiol. Behav.* **56**, 785–788.
- Bermejo, R. & Zeigler, H. P. (2000) *Somatosens. Motor Res.* **17**, 373–377.
- Ventakachalam, S., Fee, M. S. & Kleinfeld, D. (1999) *J. Neurosci. Methods* **90**, 37–46.
- Shuz, A. & Palm, G. (1989) *J. Comp. Neurol.* **286**, 442–455.
- Carvell, G. E., Simons, D. J., Lichtenstein, S. H. & Bryant, P. (1991) *Somatosens. Motor Res.* **8**, 159–164.
- Mardia, K. V., Kent, J. T. & Bibby, J. M. (1979) *Multivariate Analysis* (Academic, San Diego).
- Schmidt, M. F. & Konishi, M. (1998) *Nat. Neurosci.* **1**, 513–518.
- Seidemann, E., Zohary, E. & Newsome, W. T. (1998) *Nature* **394**, 72–75.
- Isa, T. & Kobayashi, Y. (2004) *Prog. Brain Res.* **143**, 299–305.
- Baker, S. N., Olivier, E. & Lemon, R. N. (1997) *J. Physiol. (London)* **501**, 225–241.
- Baker, S. N., Kilner, J. M., Pinches, E. M. & Lemon, R. N. (1999) *Exp. Brain Res.* **128**, 109–117.
- Fanselow, E. E. & Nicolelis, M. A. L. (1999) *J. Neurosci.* **19**, 7603–7616.
- Castro-Alamancos, M. A. & Connors, B. A. (1996) *J. Neurosci.* **16**, 2767–2779.
- Roy, S. A. & Alloway, K. D. (2001) *J. Neurosci.* **21**, 2462–2473.
- Fries, P., Reynolds, J. H., Rorie, A. E. & Desimone, R. (2001) *Science* **291**, 1560–1563.
- Roelfsema, P. R., Engel, A. K., Konig, P. & Singer, W. (1997) *Nature* **385**, 157–161.
- Kleinfeld, D., Berg, R. W. & O'Connor, S. M. (1999) *Somatosens. Motor Res.* **16**, 69–88.
- Zwied, M., Bagdasarian, K. & Ahissar, E. (2003) *Neuron* **40**, 621–630.
- Ahrens, K. F., Levine, H., Suhl, H. & Kleinfeld, D. (2002) *Proc. Natl. Acad. Sci. USA* **99**, 15176–15181.
- Singer, W. & Gray, C. M. (1995) *Annu. Rev. Neurosci.* **18**, 555–586.
- Zohary, E., Shadlen, M. N. & Newsome, W. T. (1994) *Nature* **370**, 140–143.
- Bair, W., Zohary, E. & Newsome, W. T. (2001) *J. Neurosci.* **21**, 1676–1697.
- Romo, R., Hernandez, A., Zainos, A. & Salinas, E. (2003) *Neuron* **38**, 649–657.